



HAL
open science

**Development of an isotopic oxygen exchange setup
operating under high pressure: preliminary
measurements performed on $\text{Ln}_2\text{NiO}_{4+\delta}$ (Ln=La,
Pr, Nd, MIEC) oxides**

Aurélien Flura, Jérôme Laurencin, Sébastien Fourcade, Fabrice Mauvy,
Vaibhav Vibhu, Jean-Paul Salvetat, Julie Mougin, Jean-Marc. Bassat

► **To cite this version:**

Aurélien Flura, Jérôme Laurencin, Sébastien Fourcade, Fabrice Mauvy, Vaibhav Vibhu, et al.. Development of an isotopic oxygen exchange setup operating under high pressure: preliminary measurements performed on $\text{Ln}_2\text{NiO}_{4+\delta}$ (Ln=La, Pr, Nd, MIEC) oxides. ECS Transactions, 2021, 103 (1), pp.1319-1330. 10.1149/10301.1319ecst . hal-03343009

HAL Id: hal-03343009

<https://hal.science/hal-03343009>

Submitted on 13 Sep 2021

HAL is a multi-disciplinary open access archive for the deposit and dissemination of scientific research documents, whether they are published or not. The documents may come from teaching and research institutions in France or abroad, or from public or private research centers.

L'archive ouverte pluridisciplinaire **HAL**, est destinée au dépôt et à la diffusion de documents scientifiques de niveau recherche, publiés ou non, émanant des établissements d'enseignement et de recherche français ou étrangers, des laboratoires publics ou privés.

Development of an isotopic oxygen exchange setup operating under high pressure: preliminary measurements performed on $\text{Ln}_2\text{NiO}_{4+\delta}$ (Ln=La, Pr, Nd) MIEC oxides

A. Flura^a, J. Laurencin^b, S. Fourcade^a, F. Mauvy^a, V. Vibhu^c,
J-P. Salvetat^d, J. Mougin^b and J-M. Bassat^{a,*}

^a CNRS, Univ. Bordeaux, Bordeaux INP, ICMCB, UMR 5026, F-33600 PESSAC, FRANCE

^b Univ. Grenoble Alpes - CEA/LITEN, 17 Rue des martyrs, F-30854 GRENOBLE, FRANCE

^c Institute of Energy and Climate Research, Fundamental Electrochemistry (IEK-9), Forschungszentrum Jülich GmbH, 52425 JÜLICH, GERMANY

^d CNRS, Univ. Bordeaux, PLACAMAT, UMS 3626, F-33600 PESSAC, FRANCE

**Corresponding author*

Abstract

Mixed Ionic Electronic Conductors (MIECs) used as oxygen electrodes in Solid Oxide Cells are characterized by both high oxygen diffusion (D) and surface exchange (k) coefficients. To date, the reported experiments have been performed at ambient pressure and even below. However, to reach a higher efficiency at the system level, it would be helpful to operate the Solid Oxide Electrolysers under high pressure. In this work, we describe preliminary investigations to assess the oxygen reduction/oxidation and the transport properties of the electrode materials when submitted to high pressure. We describe in detail an innovative setup that was designed to operate up to a total pressure of 50 bar. This setup has been used to characterize the properties of nickelates with MIEC properties. Oxygen exchanges were performed in the range $500 < T^\circ\text{C} < 700$, under $p(\text{O}_2) \sim 6.5$ bars. Preliminary results (oxygen over-stoichiometry, D^* and k^* coefficients) obtained on $\text{Ln}_2\text{NiO}_{4+\delta}$ (Ln=La, Pr, Nd) oxides are presented and discussed.

Introduction

There is nowadays a growing need of clean and sustainable energy sources. Due to the intermittency of renewable energies, new solutions for energy storage are required, in particular to match the fluctuations between the demand and the production. In this frame, hydrogen is considered as one of the most relevant energy vectors [1]. For its production at low cost and high efficiency, the High Temperature Steam Electrolysis (HTSE), based

on the Solid Oxide Electrolysis Cells (SOEC) technology, appears as a promising and attractive technical solution [2]. Nevertheless, hydrogen has to be stored or distributed at high pressure. Since the compression of liquid water consumes much less energy than gaseous hydrogen, it can be advantageous to perform the steam electrolysis directly under pressure [3]. Moreover, the high-temperature co-electrolysis of steam and carbon dioxide enables to convert electricity into a syngas of carbon monoxide and hydrogen [2, 4]. This syngas can be further transformed in liquid or gaseous hydrocarbons with conventional catalytic processes working at high pressure between 10 and 100 bars [5]. In this case, it has been shown that an integrated system working directly under pressure could also be energetically favored [6, 7]. In this context, it is essential to investigate the impact of high pressure on the electro-catalytic properties of the electrode materials that control the cell electrochemical response, especially the oxygen electrode.

Mixed Ionic Electronic Conductors (MIEC) are commonly used as oxygen electrodes in SOEC cells. In addition to a high electronic conductivity, the electrodes require both high oxygen diffusivity (D) and surface exchange coefficient (k) at the considered operating temperatures. Among different candidates substitutes to oxygen deficient perovskites such as $\text{La}_{0.4}\text{Sr}_{0.6}\text{Co}_{0.8}\text{Fe}_{0.2}\text{O}_{3-\delta}$ (LSCF), a second type of MIEC concerns over-stoichiometric oxides, such as nickelates $\text{Ln}_2\text{NiO}_{4+\delta}$ ($\text{Ln} = \text{La, Pr, Nd}$) [8, 9], belonging to the so-called Ruddlesden series $\text{Ln}_{n+1}\text{Ni}_n\text{O}_{3n+1}$ (here with $n=1$). These compounds with the K_2NiF_4 -type layered structure have shown promising oxygen electrode performance because of their large anionic bulk diffusion and surface exchange coefficients, combined with a good electrical conductivity and a thermal expansion coefficient matching with those of other cell components [10, 11].

To date, the reported measurements of D and k in the literature have been performed at ambient pressure and even below, whatever the considered material. Therefore, the objectives of the current work consist in: 1) performing isotopic oxygen exchanges on dense pellets with $\text{Ln}_2\text{NiO}_{4+\delta}$ ($\text{Ln} = \text{La, Pr, Nd}$) compositions under high oxygen pressure, 2) checking that the resulting oxygen over-stoichiometry δ was significantly changed after such an exchange and 3) evaluating the consequence of δ variation on D and k coefficients.

Experimental

Samples preparation

Oxygen exchange experiments require dense samples in pure materials with a compacity of at least 95%. In this study, we prepared pellets of lanthanide nickelates reaching these requisites, with a diameter of roughly 20 mm after sintering.

Pure powders of the three lanthanide nickelates were produced using the modified Pechini method [12] from Pr_6O_{11} (Aldrich chem, 99.9%), La_2O_3 and Nd_2O_3 (Strem Chemical, 99.99%) and $\text{Ni}(\text{NO}_3)_2 \cdot 6\text{H}_2\text{O}$ (Acros Organics, 99%) precursors. The final annealing was performed at 1200 °C for 12 h in air, leading to well crystallized phases. The obtained powders were ground with zirconia balls and ethanol for 4 h with the aim to obtain a mean particle size of about 0.6 μm (as determined by laser diffraction analysis). The purity of the powder was controlled by X-ray Diffraction (XRD) analysis. The materials were then sintered at 1350 °C for 4 h in order to get dense pellets.

The dense pellets were first mirror polished, using abrasives of decreasing grain diameter, then diamond paste to complete the work. Finally, cubes of roughly 4 mm side length were cut from the pellet, using a diamond cutting-disc (Isomet Buehler), in order to ensure that our samples are comparable.

Development of the specific (high pressure) oxygen exchange setup

The isotopic oxygen exchange setup (Fig.1) was developed with the aim to resist to an operating pressure under oxygen up to 40 bars. This specification requires the use of degreased stainless steel for the tubing. One line of the setup is dedicated to pumping: a vacuum of roughly 10^{-6} mbar is obtained using a turbomolecular pump. The marked ^{18}O gas is routed through another line, from a gas (air) cylinder provided by Euriso-top company with the following specifications: 1L, P = 20 bar, being the ^{16}O of air changed by ^{18}O with purity close to 98%. Another line is dedicated to ^{16}O from the laboratory. A fourth line is dedicated to cryo-pumping of the marked ^{18}O at the end of the exchange, which is achieved by immersing an one meter stainless steel rod into liquid helium. The

gas may then be used for another experiment, provided that the ratio $^{18}\text{O}/^{16}\text{O}$ is still high. Two manometers read respectively the low and high pressures.



- Ceramic tube
- HT rolling furnace
- Gas panel ($^{16}\text{O}_2$, $^{18}\text{O}_2$)
- High pressure manometers
- Cryo-pumping (liquid He) for $^{18}\text{O}_2$ recovering

Fig.1 – Overview of the original isotopic exchange device for operating up to $P = 50$ bar and $T=1100^\circ\text{C}$

The sample holder (Fig.2) is a closed cylinder built in magnesium doped zirconia: it was designed to withstand both stationary high pressure and high temperature steady state and also quick thermal quenching. It resisted through all our experiments, up to a starting quenching temperature of 800°C down to room temperature. A sliding oven mounted on rails produces the thermal quenching.



« Visible » thermal gradient just after the quenching step

Fig.2 – Mg-doped zirconia ceramic glove designed for the isotopic oxygen exchange setup operating at high pressure and temperature (approximate length and internal diameter: 20 cm and 1.5 cm, respectively)

In order to assure that the setup is gastight, a polished copper ring is pressed between the zirconia cylinder and the stainless-steel head, using six screws carefully tightened with a torque wrench.

A platinum grid introduced inside the zirconia cylinder allows precisely placing the sample in the oven hot zone. A fine gold grid was added between platinum and lanthanide nickelates to avoid the chemical reaction we observed during the first experiment at high temperature.

Oxygen exchange experiments

After placing the samples in the zirconia cylinder, the gas tightness of the setup was verified by pumping all the gas in the setup and checking that a vacuum of roughly 10^{-6} mbar was reached.

As a first step, the samples were equilibrated at the target temperature (600 °C for instance) in $^{16}\text{O}_2$ for a period at least ten times longer than the one chosen for the oxygen exchange experiment, then quenched down to room temperature. This treatment creates the baseline in $^{18}\text{O}/^{16}\text{O}$ inside the sample that will be used as reference later during the TOF-SIMS analyses. Besides, it fixes the chemistry of the materials in the bulk: for instance, the oxygen over-stoichiometry of the lanthanide nickelate. Another interest of this preliminary experiment is to determine with accuracy the pressure of gas needed at room temperature to reach 30 bars at the studied temperature.

Next, the gas was pumped and replaced with the desired pressure of $^{18}\text{O}_2$ at room temperature. The samples were quickly heated to reach the target temperature, and the oxygen exchange experiments carried out for a determined time. Samples were then quenched down to room temperature, and $^{18}\text{O}_2$ recovered using liquid helium. Finally, the samples were taken out of the zirconia cylinder to be prepared for the TOF-SIMS analyses.

A correction on the exchange time, related to the duration needed to reach the target temperature and then to quench the samples, was applied using the Killoran correction [13].

Thermogravimetric analyses

Our first goal was to determine the delta (δ) value characterizing the oxygen over-stoichiometric nickelates (with general formulation $\text{Ln}_2\text{NiO}_{4+\delta}$), after each thermal treatment performed under pressure followed by a thermal quenching. For this purpose, TGA experiments were carried out using a TA Instrument[®] TGA-5500 device. First, the dense bar samples of nickelates (after exchange experiments) were crushed into powder using mortar-pestle. Then the powders were heated under air up to 150 °C/1h, then cooled down to room temperature with a slow rate (2 °C.min⁻¹), with the aim to remove any traces of water. Then, a second cycle was performed under Ar - 5% H₂ flux with a very slow heating rate of (0.5 °C.min⁻¹) up to 1000 °C. The full decomposition of the material under reducing atmosphere leads to the determination of the oxygen stoichiometry after cycling the sample down to room temperature. The decomposition products (Ln₂O₃ and metallic Ni) were verified by XRD after the thermal cycle. An example of a thermal cycle recorded under Ar/5% H₂, on Nd₂NiO_{4+ δ} after isotopic exchange performed under oxygen pressure is given in Fig.3.

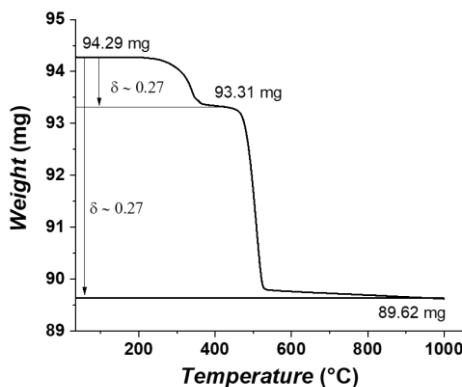


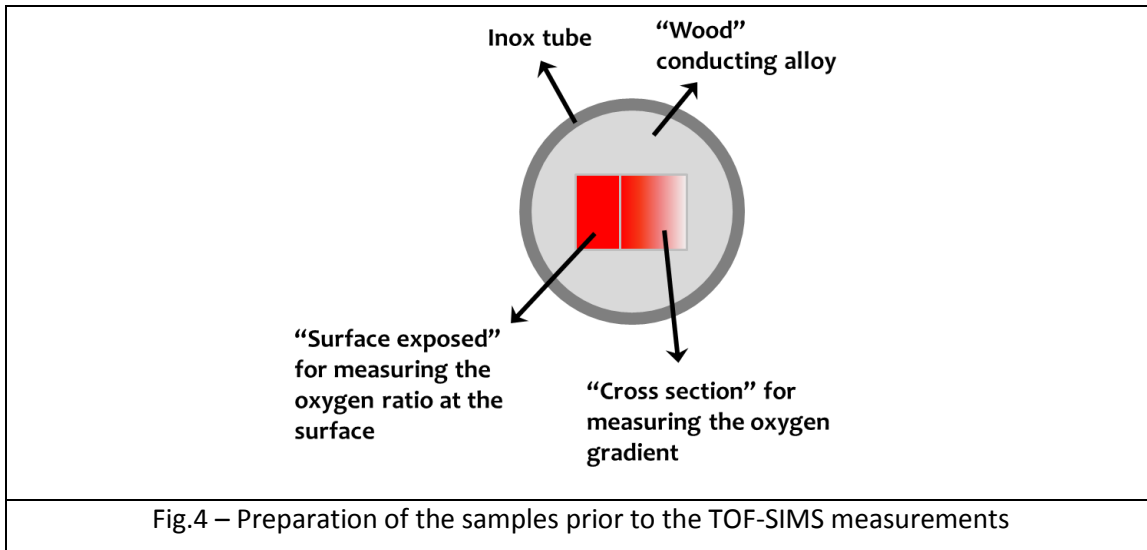
Fig.3 – TGA experiment performed under Ar/5% H₂ flow (heating rate 2°C.min⁻¹), on a Nd₂NiO_{4+ δ} sample (powder crushed from a dense pellet), after the oxygen isotopic exchange step performed at 600°C during 18.600s under pO₂ = 6,5 bar. The graph shows the mass evolution vs. T°, the calculations of delta are explained below in the text

ToF-SIMS analyses

Samples preparation

The cubes were cut in half with the utmost care using the diamond cutting-disc. This cut is necessary to reveal the gradient in ¹⁸O. The new face created was then mirror polished.

The resulting two samples were pressed altogether in a way detailed thereafter and fixed inside a stainless-steel ring with Wood alloy (*cf.* Fig 4). The particularity of this preparation is that one of the samples exposes the surface of the cube that was in direct contact with $^{18}\text{O}_2$, while the other sample exposes the bulk of the cube that contains the gradient of ^{18}O .



The benefit of this setup is to measure with precision the ratio $^{18}\text{O}/^{16}\text{O}$ at the surface of the sample, averaged over a large area. This value is used as the origin of the gradient measured on the other sample.

TOF-SIMS analyses

SIMS experiments were performed using a TOF SIMS 5 (IONTOF, Münster, Germany). Samples were analysed in spectroscopy mode by scanning a primary 30 keV Bi^+ beam over $500 \times 500 \mu\text{m}^2$ area, interlaced with a 1 keV Cs^+ sputter beam scanned over $600 \times 600 \mu\text{m}^2$ to eliminate surface impurities and enhance production of negative secondary ions. Area of interest was adjusted using the integrated optical camera and sample stage controls so that a sample edge was located vertically on the right or left of the raster field of view. Data acquisition was started in the 3D mode, and the following procedure was used to determine the stopping condition: once the secondary ions of interest (e.g. ^{18}O and ^{16}O) peaks were selected on the spectra subpanel, images of ion

intensity with definition 256 x 256 pixels were automatically generated by the instrument software (SurfaceLab 7) in the image stockpile subpanel. The images of ^{18}O and ^{16}O intensities are then combined to generate an image of the isotopic ratio of interest $I(^{18}\text{O})/(I(^{18}\text{O})+I(^{16}\text{O}))$, and performed an average linescan thereof using the X-area feature of SurfaceLab linescan editor. Using this procedure we could follow the gradient line-scan progress in real-time so that data acquisition could be stopped, typically after 5 to 10 min, when the gradient was stabilized at a good S/N ratio. Doing so an isotopic ratio profile averaged over a volume of approx. $500 \times 500 \times 0.1 \mu\text{m}^3$ is generated, which minimizes artifacts from impurities and inhomogeneities. The data were finally exported as ASCII file for further analysis. In some cases, ^{18}O gradient spanned over $500 \mu\text{m}$ so that a second adjacent area was analysed similarly and stitched to the previous one. The experimental oxygen profiles (evolution of $I(^{18}\text{O})/I(^{18}\text{O})+I(^{16}\text{O})$ vs. depth) were then fitted using the Crank solution to the equation of the second Fick's law of gas diffusion in solids [14, 15], which leads determining the D^* and k^* coefficients (* being relative to the diffusion of the ^{18}O tracer).

Results and discussion

Summary of the oxygen isotopic exchange conditions

Table 1 gathers the temperatures and time durations used for the isotopic exchanges. For a given temperature, three pellets (one for each studied composition) were used together.

Table 1. Temperatures and duration times used for the oxygen exchange steps

Oxygen exchange temperature ($^{\circ}\text{C}$)	Oxygen exchange time (s)
500	78720
550	23700
600	18600
650	12540
700	4920 / 2520

Determination of the oxygen over-stoichiometry's of the studied samples after the oxygen exchange steps

After the oxygen exchange steps, the samples were quenched to stop the oxygen diffusion phenomenon and to keep the oxygen composition that the oxide reached in the used experimental conditions. Our first goal was to determine the corresponding oxygen over-stoichiometry values and, for this purpose, we used TGAs experiments performed under reducing atmosphere (Ar/5% H_2 flow) on powders (crushed pellets). As evidenced on Fig. 3, the decomposition of the oxide is occurring in two steps: 1) At intermediate temperature a first plateau is evidenced, which corresponds to the stabilization of the oxide only containing Ni^{+II} , *i.e.* a composition $Ln_2NiO_{4.0}$ ($Ln=La, Pr, Nd$). The measured weight loss between room temperature and this temperature corresponds exactly to the disappearance of the oxygen over-stoichiometry δ ; 2) in a second step, at higher temperature the full decomposition of the oxide is observed, leading as checked by XRD to the formation of Ln_2O_3 *plus* metallic Ni. Measuring the weight loss recorded between room temperature and the full reduction is then a second way to determine δ . Table 2 gathers the results obtained for each exchanged sample, the given value is an average between the two calculations detailed above.

Table 2. Oxygen over-stoichiometries values determined by TGAs experiments performed under reducing atmosphere, on the different samples previously exchanged under ^{18}O atmosphere, at a given temperature, under $pO_2 = 6,5$ bar

Exchange T°C	$La_2NiO_{4+\delta}$	$Pr_2NiO_{4+\delta}$	$Nd_2NiO_{4+\delta}$
500	$\delta = 0,25$	$\delta = 0,31$	$\delta = 0,29$
550	-	$\delta = 0,33$	$\delta = 0,27$
600	$\delta = 0,21$	$\delta = 0,43$	$\delta = 0,27$
650	-	$\delta = 0,36$	$\delta = 0,28$
700	$\delta = 0,23$	$\delta = 0,5$	$\delta = 0,28$

As a preliminary result and as expected, whatever the temperature used for the oxygen exchange all the samples exhibit a significant increase of oxygen over-stoichiometry after the thermal treatment performed under oxygen pressure, compared to the value obtained after the chemical synthesis. Indeed, let us recall the compositions determined at room temperature after the synthesis performed in air: $La_2NiO_{4.16}$, $Pr_2NiO_{4.22}$ and $Nd_2NiO_{4.21}$. There is a large agreement in the literature regarding these values (see, for instance, [16]

and the joined references). Note that under air and atmospheric pressure, such over-stoichiometry slightly decreases upon heating (for instance, for Ln=Nd, the measured composition is Nd₂NiO_{4.13} at 700°C [16]). Such evolution was also expected on the current results (the higher the exchange temperature, the lower the δ value should be). However, this conclusion is difficult to draw when considering the results gathered in table 2. However, the exchange duration times were different depending on the temperature (to ensure a partial diffusion of the ¹⁸O gas in the ceramic the exchange time is lower for higher temperatures), which could partly explain this result. Another questionable point is the observed scattering of the δ values regarding Pr₂NiO_{4+ δ} , being this material the most oxidized one.

Finally, at this stage our conclusion is that the three studied compositions are significantly over-oxidized after the thermal treatments performed under ¹⁸O pressure, and that we will be able to evaluate the changes in δ on the D* and k* coefficients.

Oxygen diffusion profiles and determination of the D* and k* coefficients on samples treated under high ¹⁸O

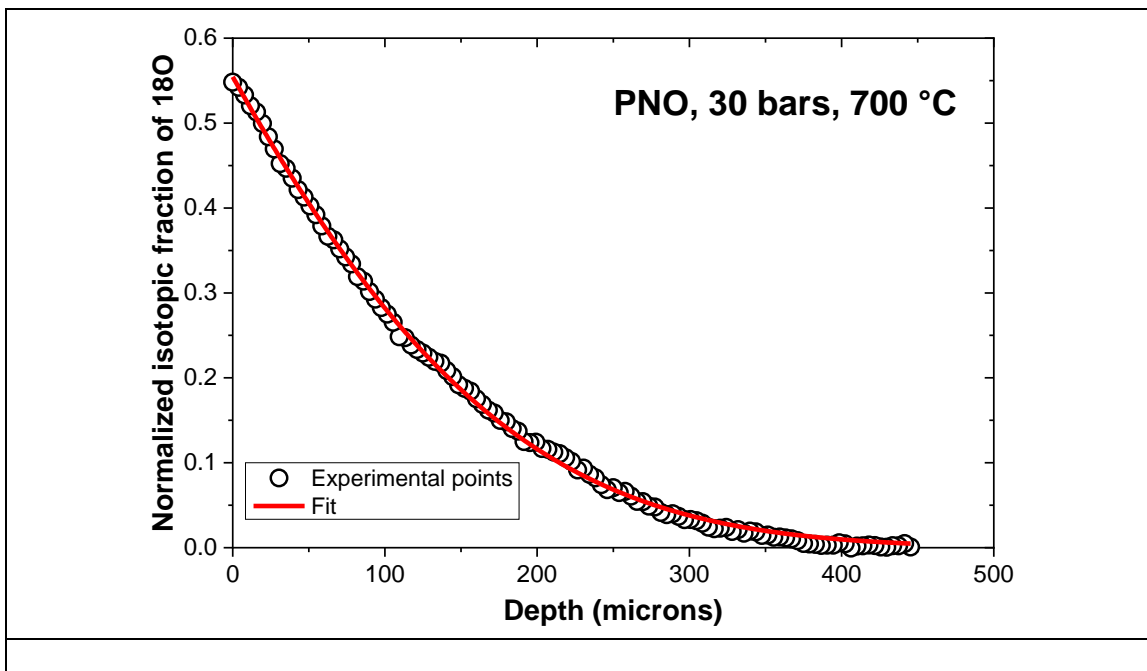


Fig.5 – Gradient in ¹⁸O/¹⁶O measured on Pr₂NiO_{4+ δ} (PNO) cross-section after oxygen exchange experiment performed in air at 700 °C, P_{total} = 30 bar (PO₂ ~ 6,5 bar) for 4920s.

Fig.5 is an example of oxygen profile recorded on $\text{Pr}_2\text{NiO}_{4+\delta}$ at 700°C after an exchange performed under total pressure of air $P_{\text{tot}} = 30$ bar ($\text{PO}_2 \sim 6.5$ bar).

Fig. 6, 7 and 8 plot the evolutions of the D^* and k^* coefficients vs. T , on the over-oxidized materials, *i.e.* $\text{La}_2\text{NiO}_{4+\delta}$, $\text{Pr}_2\text{NiO}_{4+\delta}$ and $\text{Nd}_2\text{NiO}_{4+\delta}$, respectively.

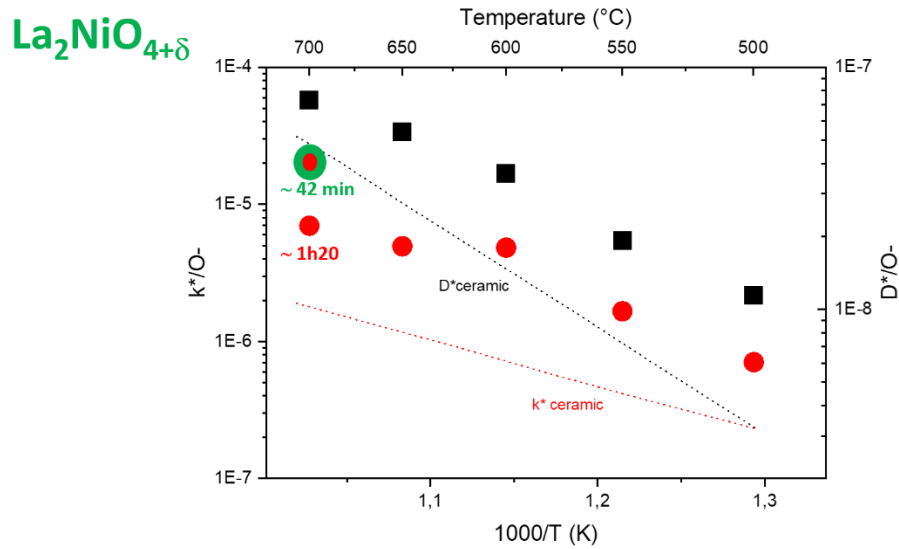


Fig.6 – Evolutions as a function of temperature of the k^* (red dots) and D^* (black dots) coefficients for over-oxidized $\text{La}_2\text{NiO}_{4+\delta}$ samples (table 2). The red and black dashed lines give respectively the corresponding k^* and D^* data for isotopic exchanges performed under $p\text{O}_2 = 0.2$ bar (from [10])

The k^* plot of $\text{La}_2\text{NiO}_{4+\delta}$ was quite peculiar, and we suspected that the high temperature values were erroneous. Indeed, the exchange rate largely increases with the temperature, and it is easy to saturate the surface of our sample with ^{18}O if the exchange time is too long. In this case, the measured value of k^* will be false. Then, we reduced the exchange time at 700°C from 80 min down to 42 min : we measured a k^* value that is close to the linear regression plot of the k^* values obtained at 500°C , 550°C and 600°C .

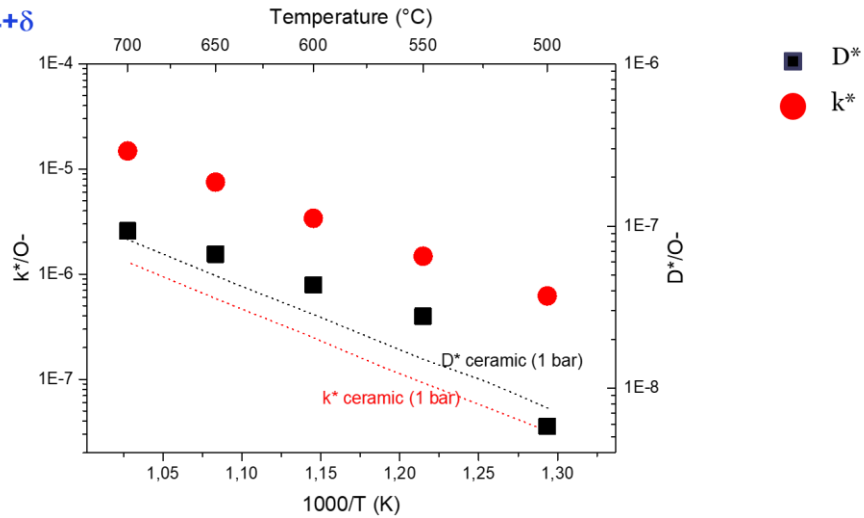


Fig.7 – Evolutions as a function of temperature of the k^* (red dots) and D^* (black dots) coefficients for over-oxidized $\text{La}_2\text{NiO}_{4+\delta}$ samples (table 2). The red and black dashed lines give respectively the corresponding k^* and D^* data for isotopic exchanges performed under $p\text{O}_2 = 0.2$ bar (from [10])

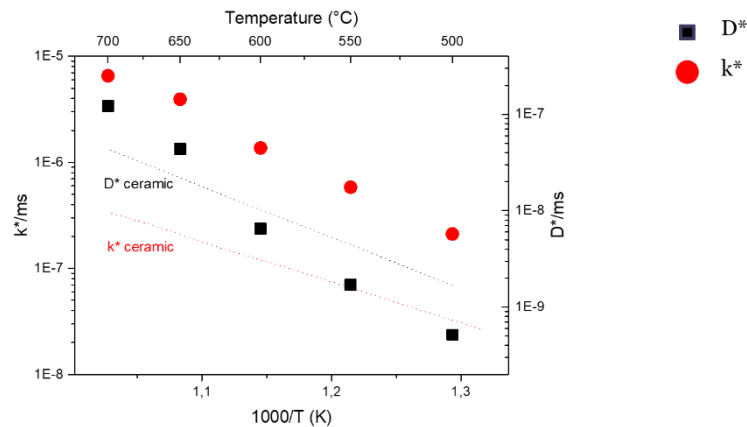


Fig.8 – Evolutions as a function of temperature of the k^* (red dots) and D^* (black dots) coefficients for over-oxidized $\text{La}_2\text{NiO}_{4+\delta}$ samples (table 2). The red and black dashed lines give respectively the corresponding k^* and D^* data for isotopic exchanges performed under $p\text{O}_2 = 0.2$ bar (from [10])

As a first comment, whatever the considered material both D^* and k^* coefficients are improved after oxygen exchanges performed under pressure compared to the corresponding values obtained after oxygen exchange performed under $p\text{O}_2 = 0.2$ atm. The ionic transport properties of such MIEC materials will be then probably improved in the case of a SOEC operation under pressure (the measurements are in progress). It is of

course a very interesting result leading to carefully consider these innovative oxygen electrodes for the application.

A second comment is that the D^* coefficient is less improved compared to the k^* coefficient, whatever the composition, again. Some years ago Chronopoulos et al. [17], then Parfitt et al. [18] have performed Molecular Dynamics (MD) simulations regarding the oxygen diffusion in $\text{La}_2\text{NiO}_{4+\delta}$ and $\text{Pr}_2\text{NiO}_{4+\delta}$, respectively. The dominant mechanism of oxygen transport is *via* the network of apical oxygen sites connected by interstitial ion sites along a two-dimensional network (the so-called interstitialcy mechanism [17]). A continuous network of partially occupied sites necessary for bulk ionic diffusion is formed. The intermediate state where both ions are in intermediate In the article by Parfitt et al., the oxygen diffusivities were calculated for a range of hyper-stoichiometries, and an excellent agreement was found between the absolute calculated values and those observed experimentally. Initially (the first calculated point being $\delta = 0$), the diffusivity rises very quickly as a function of δ , but rapidly levels off. Between $\delta = 0.05$ and $\delta = 0.25$ the diffusivity still increases but smoothly. The increase of the formation energy of oxygen interstitials is involved by the authors, as well as a stiffening of the lattice cause by the additional oxygen interstitial pinning the NiO_6 sub-lattice, which reduces the passage of the oxygen ions. Our results are in good agreement with such calculations, indeed when increasing δ for each of the studied nickelate by means of oxygen pressure we observed a limited increase of the diffusion coefficient, while a larger one could be expected. The largest increase is observed when the initial oxygen over – stoichiometry is the lowest one, for $\text{La}_2\text{NiO}_{4+\delta}$ ($\delta = 0.16$ at room temperature after annealing under air at normal pressure).

On the opposite, within this work, we also evidenced that the kinetic constant of oxygen exchange k^* increases significantly with the pressure. Indeed, considering the reaction of oxygen insertion into the material it can be easily shown that the chemical kinetic constant k_{chem} (which is directly related to k^*) must evolve with the square root of the oxygen partial pressure. This theoretical dependence with $P(\text{O}_2)$ is thus consistent with the reported experimental results. Moreover, this increase is also in good agreement with other experiments carried at low oxygen partial pressure [19].

Conclusions

For a higher efficiency of the Solid Oxide Electrolyser devices, it is envisaged to operate them under high oxygen pressure. On another hand, oxygen over-stoichiometric nickelates with the K_2NiF_4 -type structure have been developed for several years as oxygen electrodes because being a valuable alternative to the more conventional oxygen deficient perovskites. Then the goal of this work was to determine the oxygen diffusion and surface exchange coefficients (which characterize the O^{2-} ionic conductivity) of three well known nickelates ($La_2NiO_{4+\delta}$, $Pr_2NiO_{4+\delta}$ and $Nd_2NiO_{4+\delta}$, respectively) by the IEDP method after a preliminary isotopic exchange step performed under high oxygen pressure. For this purpose, an original set-up has been developed, which is now available for future experiments performed on another kinds of materials.

As expected, the measured oxygen over-stoichiometry of the three materials is significantly increased after the oxygen isotopic exchanges performed in the temperature range $500 < T^\circ C < 700$ under $p(O_2) \sim 6.5$ bars. The measured evolutions of D^* and k^* coefficients are thus representative of materials in a very different oxidation state.

Both D^* and k^* coefficients are improved after oxygen exchanges performed under pressure compared to that performed under $pO_2 = 0.2$ atm (atmospheric condition). However, D^* is less improved compared to k^* , whatever the composition. This statement would thus indicate that the electrochemical properties of such MIEC materials are improved for a SOEC operation under pressure.

Acknowledgments

A.F. thanks the CNRS French grouping GDR HysPàc for supporting this research work *via* an internal project. CEA is acknowledged for its valuable technical aid, including the supply of the pressurized air bottle enriched in ^{18}O .

References

1. T.N. Veziroglu, F. Barbir, *Int. J. Hydrogen Energy* 17, 391 (1992).
2. S.D. Ebbesen, S.H. Jensen, A. Hauch and M.B. Mogensen, *Chem. Rev.* 114, 10697 (2014).
3. D. Todd, M. Schwager, W. Merida, *J. Power Sources* 269, 424 (2014).
4. Y. Wang, T. Liu, L. Lei, F. Chen, *Fuel Process Tech* 161, 248 (2017).
5. *Catalysis in C1 Chemistry*, Ed by W. Keim, D. Reidel Publishing company, 41 (1983).
6. E. Giglio, A. Lanza, I. M. Santarelli, P. Leone, *J. Energy Storage* 1, 22 (2015).
7. J.B. Hansen, N. Christiansen, J.U. Nielsen, *ECS Transactions* 35(1), 2941 (2011).
8. G. Amow, I. J. Davidson, S. J. Skinner, *Solid State Ionics*, **177**, 1205 (2006).
9. S. Takahashi, S. Nishimoto, M. Matsuda, M. Miyake, *Journal of the American Ceramic Society*, **93**, 2329 (2010).
10. E. Boehm, J.M. Bassat, P. Dordor, F. Mauvy, J.C. Grenier and P. Stevens; *Solid State Ionics* 176, 2717 (2005).
11. A. Aguadero, J.A. Alonso, M.J. Martinez-Lope, M.T. Fernandez-Diaz, M.J. Escudero and L. Daza, *J. Mater. Chem.* 16 (33), 3402 (2006).
12. P. Courty, H. Ajot, C. Marcilly, B. Delmon, *Powder Technology*, 7 (1) (1973) 21–38.
13. D.R. Killoran, *Journal of the Electrochemical Society* 109 (2), 170.
14. J. Crank, *The Mathematics of Diffusion*, Clarendon Press, Oxford, 2nd Edition, 1975.
15. J.M. Bassat, M. Petitjean, J. Fouletier, C. Lalanne, G. Caboche, F. Mauvy and J.C. Grenier, *Applied Catalysis A: General* 289, 84 (2005).
16. A. Flura, S. Dru, C. Nicollet, V. Vibhu, S. Fourcade, E. Lebraud, A. Rougier, J.M. Bassat, J.C. Grenier, *Journal of Solid State Chemistry* 228, 189 (2015).
17. A. Chroneos, D. Parfitt, J.A. Kilner and R.W. Grimes, *J. Mater. Chem.*, 20, 2666 (2010).
18. D. Parfitt, A. Chroneos, J.A. Kilner and R. Grimes, *Phys. Chem. Chem. Phys.* 12, 6834 (2010).
19. M. Katsuki, S. Wang, M. Dokiya, T. Hashimoto, *Solid State Ionics*, **156**, 453 (2003).